Available online at www.sciencedirect.com
ScienceDirect
Polymer 48 (2007) 6439–6447
polymer
www.elsevier.com/locate/polymer

Biodegradable poly(L-lactide)/poly(ε-caprolactone)-modified montmorillonite nanocomposites: Preparation and characterization

Zhenyang Yu [a], Jingbo Yin [a,*], Shifeng Yan [a], Yongtao Xie [a], Jia Ma [b], Xuesi Chen [b,**]

[a] *Department of Polymer Materials, Shanghai University, Shanghai 201800, PR China*
[b] *State Key Laboratory of Polymer Physics and Chemistry, Changchun Institute of Applied Chemistry, Chinese Academy of Sciences, Changchun 130022, PR China*

Received 22 March 2007; received in revised form 19 June 2007; accepted 7 July 2007
Available online 18 July 2007

Abstract

New nanocomposites were prepared by melt blending poly(L-lactide) (PLLA), poly(ε-caprolactone) (PCL), and organically modified montmorillonite (OMMT). The obtained nanocomposites showed enhanced tensile strength, modulus and elongation at break than that of PLLA/PCL blends. The dynamic mechanical analysis showed the increasing mechanical properties with temperature dependence of nanocomposites. Wide-angle X-ray diffraction analysis and transmission electron microscopy indicated that the material formed the nanostructure. Adding OMMT improved the thermal stability and crystalline abilities of nanocomposites. The morphology was investigated by environmental scanning electron microscopy, which showed that increasing content of OMMT reduces the domain size of phase-separated particles. The specific interaction between each polymer and OMMT was characterized by the Flory–Huggins interaction parameter, B, which was determined by the equilibrium melting point depression of nanocomposites. The final values of B showed that PLLA was more compatible with OMMT than PCL.

Keywords: Poly(L-lactide); Poly(ε-caprolactone); Nanocomposites

1. Introduction

With the increasing public attention to environmental problems, the research of biodegradable polymers has gained considerable momentum in recent years [1–5]. Poly(lactic acid) (PLA) and poly(ε-caprolactone) (PCL) are the most popular commercial biodegradable polymers that have found wide applications, especially in the biomedical applications [6–10]. However, both PLA and PCL have some disadvantages that restrict their practical applications. For instance, PLA has high strength and melting temperature, but it degrades relatively slow and is hard and brittle. PCL has high flexibility and relatively fast rate of degradation, but its strength is relatively low, and the 60 °C melting point is too low for many applications. Obviously, PLA and PCL have strong complementary performance.

Polymer blending is often an effective way to improve the original properties of the polymers. However, because of the fact that most polymer pairs are thermodynamically immiscible with each other, these polymer blends have poor mechanical properties. Traditionally, people can either add another component that is miscible with both parent polymers [11], or induce a chemical reaction to modify the polymer interface to enhance the compatibility between the component polymers [12].

Recent research has shown that organoclay in polymer blends could not only increase the mechanical property, the thermal stability, and the compatibilization as a kind of compatibilizer, but also decrease the gas permeability and flammability of polymer blends. Hsiao et al. [13] reported that

* Corresponding author. Tel.: +86 21 69982432.
** Corresponding author. Tel.: +86 431 85262112.
E-mail addresses: jbyin@shu.edu.cn (J. Yin), xschen@ciac.jl.cn (X. Chen).

0032-3861/$ - see front matter © 2007 Elsevier Ltd. All rights reserved.
doi:10.1016/j.polymer.2007.07.024

the addition of organoclays resulted in a drastic reduction in the average microdomain sizes of a polystyrene/poly(methyl methacrylate) blend. Fu et al. showed that immiscible polystyrene and polypropylene chains could partially intercalate into the gallery of OMMT, and that parts of the chains located outside the gallery served as a compatibilizer like a block copolymer, which promoted the compatibilization process [14]. Choi et al. [15] prepared poly(ethylene oxide)/poly(methyl methacrylate) blends and calculated the Flory–Huggins interaction parameters, B, to reveal the degree of interaction between polymers and OMMT. Recently, Yoon et al. [16] investigated the 'compatibilization-like' effect of twice-functionalized organoclay (TFC) on poly(L-lactide)/poly(butylene succinate) blends in detail. The result showed that TFC could enhance the compatibility of blend so that the TFC-modified blend was highly compatible with PLLA.

Previous researches have proved that organoclay could act as compatibilizers in the immiscible polymer blends. However, very few studies have investigated the mechanical properties and the thermal stabilities of final products. Our research has referred these two substantial properties not only to reveal its common characters but also for further applications of this kind of nanocomposites. The research of microstructure of nanocomposites exposed that OMMT can reduce the phase-separated degree. Furthermore, the thermodynamic interaction energy density, B, was calculated to describe the interaction between polymer and organoclay. This method is based on the well-known Nishi–Wang equation for the equilibrium melting point depression of miscible polymer blends [17].

2. Experimental section

2.1. Materials

Poly(L-lactide) (PLLA) ($M_w = 1.95 \times 10^5$) was purchased from Nature Works LLC, USA. The poly(ε-caprolactone) (PCL) ($M_w = 7 \times 10^4$) was kindly supplied by Zhejiang Hisun Pharmaceutical Co., Ltd., China. Organophilic montmorillonite (OMMT, I.34TCN) was obtained from Nanocor, Inc., USA, which was modified with bis-(2-hydroxyethyl) methyl (hydrogenated tallowalkyl) ammonium cations.

2.2. Preparation of nanocomposites

PLLA and PCL were dried overnight at 60 °C and 40 °C under vacuum, respectively, to remove residual water. The OMMT was also dried at 40 °C under reduced pressure for 8 h. Blending of PLLA and PCL (the weight ratio of PLLA: PCL = 90:10) with OMMT was performed on a counter-rotating mixer with a rotation speed of 32 rpm for 5 min, then at 64 rpm for 5 min. The processing temperature was set at 180 °C but it increased to 185 °C upon mixing. Products were hot pressed at 180 °C under 20 Mpa for 3 min to prepare sheets with a thickness of approximately 1.0 mm. The sheets were then cooled down by being compressed at room temperature under 20 Mpa for 20 min.

2.3. Characterization

2.3.1. Tensile testing

Dumbbell-shaped tensile test specimens with effective dimensions of 25 mm × 6 mm × 1.0 mm were prepared by pneumatic-controlled impact shaping machine. Normal tensile tests were conducted on a D&G DX-10000 electronic tensile tester at the speed of 50 mm/min at room temperature. The tensile strength, elastic modulus and elongations at break were obtained by averaging over five specimens.

2.3.2. Dynamic mechanical analysis

Dynamic mechanical properties of nanocomposites were measured by MAK-04 Viscoanalyser of Metravib Co., France, in the tension–torsion mode. The temperature dependence of dynamic storage modulus (G'), loss modulus (G'') and their ratio ($\tan\delta$) were conducted at a constant frequency (ω) of 6.28 rad/s with the strain amplitude of 0.05% and in the temperature range of −20 to 160 °C with heating rate of 2 °C/min.

2.3.3. X-ray diffraction

WAXD experiments were performed on a diffractometer (D/MAX2550, Rigaku, Japan) using Cu Kα radiation (wavelength, 1.54 Å) at room temperature in the range of $2\theta = 2$–30° with scanning rate of 2 °C/min.

2.3.4. Environmental scanning electron microscopy

The morphologies of the fracture surfaces of nanocomposites were examined by XL-30 ESEM FEG, Philips, in 15–20 kV accelerating voltage (Tungsten filament). The samples were fractured in liquid nitrogen and covered by gold vapors.

2.3.5. Transmission electron microscopy

The morphologies of the clay dispersion were investigated by JEM-2010, JEOL, Japan, in 100 kV accelerating voltage (Tungsten filament). The sample was deposited on carbon-coated copper grids after microtomed by the Leica CM1100 Cryostat Microtome (Swiss) with a diamond knife.

2.3.6. Thermogravimetric analysis

TGA was performed using a simultaneous thermal analysis STA 409 PC from Netzsch with a heating ramp of 20 °C/min under air flow (60 ml/min) from room temperature to 600 °C.

2.3.7. Differential scanning calorimeter

The thermal parameters of PLLA/PCL blend and the nanocomposites were measured by DSC-7, Perkin–Elmer, under nitrogen flow with a heating rate of 10 °C/min from 0 °C to 200 °C. DSC 200 PC, Netzsch, was used to measure the equilibrium melting temperature (T_m^0). For PLLA/OMMT system, the sample was heated to 190 °C (PCL/OMMT was 90 °C), and maintained at that temperature for 5 min to make sure that the polymer crystals were melted completely. Then the sample was quenched to the crystallization temperature T_c by liquid nitrogen, held at that temperature for at least 30 min to ensure complete crystallization. At last, the sample was heated at the heating rate of 20 °C/min.

3. Results and discussion

3.1. Mechanical properties

3.1.1. Tensile properties

The tensile properties of polymeric materials can be improved in different degrees if nanocomposites are formed with layered silicates. The tensile strengths of hybrid films with different OMMT contents are presented in Fig. 1(a). The figure shows that low contents of OMMT (1 wt% in figure) can increase the tensile strength whereas high OMMT contents in nanocomposites will cause the material to become brittle. Fig. 1(b) represents the tensile modulus of nanocomposites. The tensile modulus increases with the increase of OMMT contents and possesses a maximum value for the critical OMMT loading 3 wt%. The enhancement of the modulus of nanocomposites at such low clay concentrations, comparing with the normal fillers, cannot be attributed simply to the introduction of higher modulus inorganic filler. As high aspect ratio of clay, the surface area exposed to the polymer is huge, the region of the polymer matrix is physisorbed on the silicate surface, and is thus stiffened though its affinity for and adhesion to the filler surfaces [18]. When continuing to increase the OMMT contents, the modulus of the nanocomposites started to decrease. The elongations at break of the nanocomposites are shown in Fig. 1(c). To compare with the PLLA/PCL blend, the elongation at break of 1% OMMT nanocomposites increased about 30%.

Fig. 2 is the stress–strain curve of pure PLLA, PLLA/PCL and PLLA/PCL/1% OMMT. From this figure the effect of adding PCL and OMMT can be seen clearly and directly. PCL can make the brittle PLLA be a flexile material whereas the strength loses largely and the strength and toughness of the nanocomposite with 1 wt% OMMT become better than those of the PLLA/PCL blend. The reason of it can be seen from the digital photos of materials' break. The toughness of glassy plastics can be increased by the addition of small quantities of rubber in the form of a polymer blend [19]. PCL, the rubber-like polymer, promotes crazing in the material, which absorbs the energy locally.

3.1.2. Dynamic mechanical properties

Fig. 3 shows the temperature dependence of the dynamic mechanical properties of PLLA/PCL blend and the nanocomposites with OMMT. Adding OMMT can properly enhance the storage modulus G' and the loss modulus G'' especially when

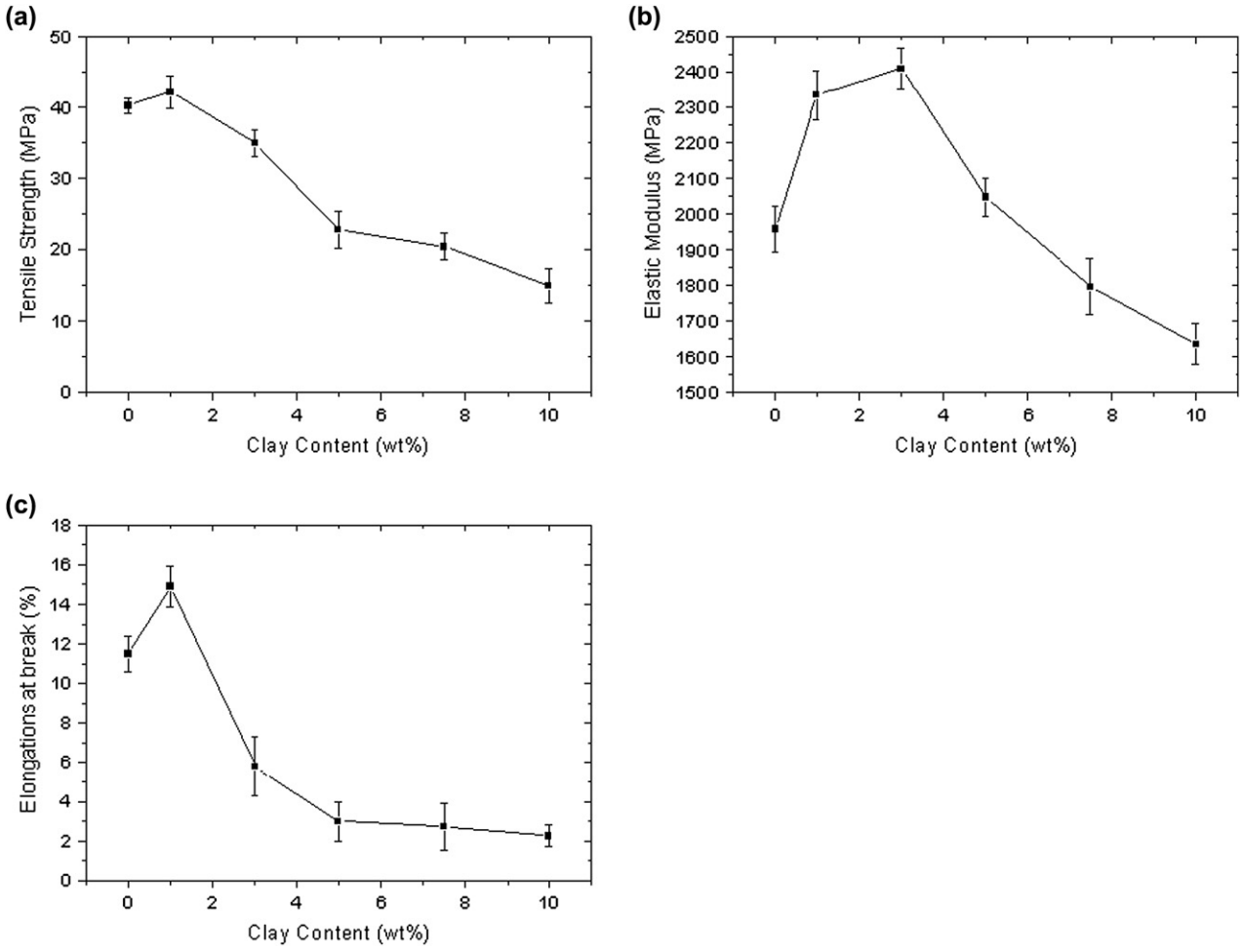

Fig. 1. Tensile strength (a), elastic modulus (b) and elongations at break (c) of PLLA(90)/PCL(10) with various contents of OMMT.

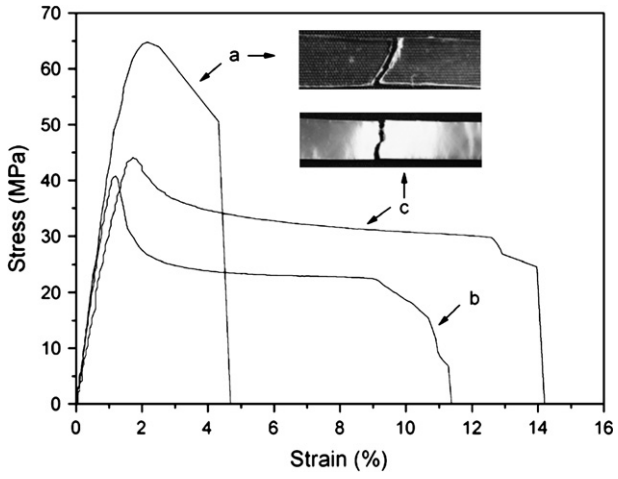

Fig. 2. Stress–strain curves of pure PLLA (a), PLLA/PCL (b) and PLLA/PCL/1% OMMT (c) and the fracture photos of PLLA and PLLA/PCL/1% OMMT.

the temperature is above the T_g. This is mainly due to not only mechanical reinforcement by clay particles but also the extended intercalation at high temperature [20]. For example, there is a G' plateau can be observed for the composites with 3% OMMT from 140 °C to 160 °C. This phenomenon shows that the composite in this OMMT loading has the best heat-resistance because of the further extent of clay intercalation and it also can be seen in other paper [21]. Below the

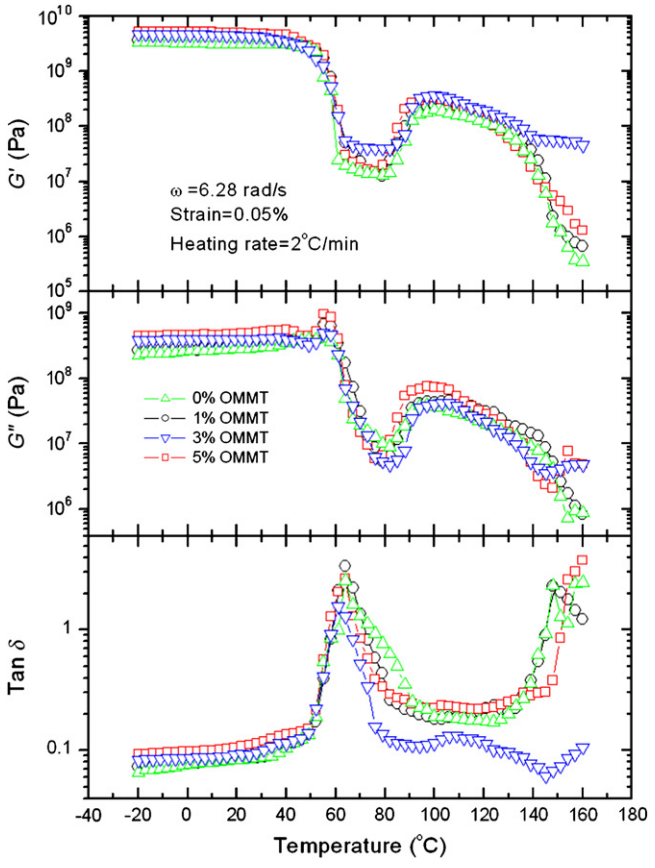

Fig. 3. Temperature dependence of storage modulus (G'), loss modulus (G'') and their ratio tan δ for pure blend and their nanocomposites.

Table 1
G' values of PLLA/PCL blend and their nanocomposites at various temperatures

Storage modulus, G' (Gpa)				
Samples	−20 °C	−40 °C	100 °C	145 °C
PLLA/PCL	3.33	3.05	0.20	0.006
With 1% OMMT	3.66	3.43	0.24	0.01
With 3% OMMT	4.64	3.44	0.35	0.06
With 5% OMMT	5.19	4.57	0.32	0.008

T_g, there is also some unapparent improvements in moduli with the increase of the OMMT content. Table 1 summarizes the G' values of all nanocomposites and the corresponding matrices without OMMT at various temperature ranges, which showed an obviously increase of G' with the addition of OMMT. For instance, compared to that of PLLA/PCL blend, the increment of G' of the nanocomposite with 5% OMMT is 50% at 40 °C and 60% at 100 °C, respectively. Noticeably, there is a dramatic increase of storage modulus and loss modulus from 80 °C and reach a peak at 100 °C approximately. This cold crystallization peak shows that this PLLA has a really excellent crystalline ability [22]. Due to the low heating rate of 2 °C/min, PLLA has enough time to form crystals which would enhance the mechanical properties of material.

From the tan δ–T curve it is found that the tan δ peak of the corresponding clay-free blend shifts to higher temperature. This may be due to the intercalation of the polymer chains into the galleries of the clay layers, which leads to the suppression of the mobility of the polymer segments near the interface. This assumption is supported by the WAXD patterns of these nanocomposites (see Fig. 5), which exhibit weak but significant peaks from the expanded (002) plane. There are also some sharp increases in curve of tan δ above 140 °C, which indicate that the main chains of macromolecule start its fluid movement in certain high temperature [23].

In conclusion, adding OMMT can improve the thermal mechanical properties of material and there is certainly no denying that these mechanical properties of nanocomposites are essential to their further applications.

3.2. Thermal stability

An obvious change in thermal stability of nanocomposites based on PLLA/PCL blend and different contents of OMMT is explicitly observed by TGA that is shown in Fig. 4 and the mass loss temperatures of 80% ($T-80\%$), 60% ($T-60\%$), 40% ($T-40\%$) and 20% ($T-20\%$) are listed in Table 2, which has a maximum clay content of 5 wt% to gain the greatest thermal stability. With the increasing amount of the OMMT, thermal stability of material decreases. This was also found by Paul et al. [24] who explained the phenomenon by the theory 'relative extent of exfoliation/delamination in function of the amount of organoclay' in 2003. When OMMT loading is less than 5 wt%, the increase of OMMT content results in relatively more exfoliated individual particles, which leads to outstanding improvement of thermal stability of nanocomposites. However, when the filling loading is beyond 5 wt%,

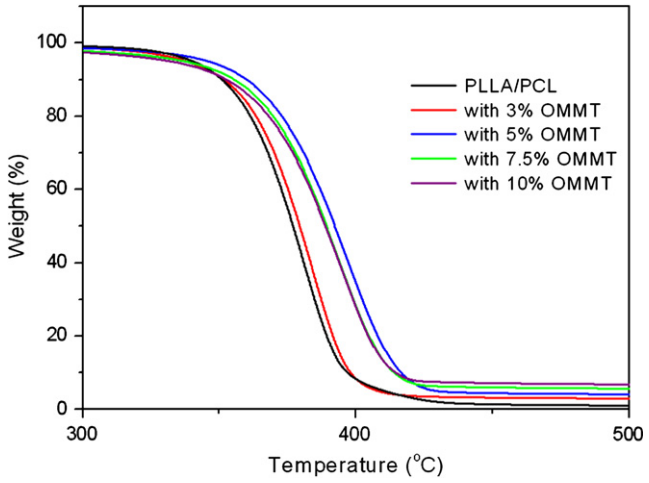

Fig. 4. Thermogravimetric analysis of PLLA/PCL blend and nanocomposites with various amounts of OMMT (experiments operated under air flow with a heating rate of 20 °C/min from 20 to 600 °C).

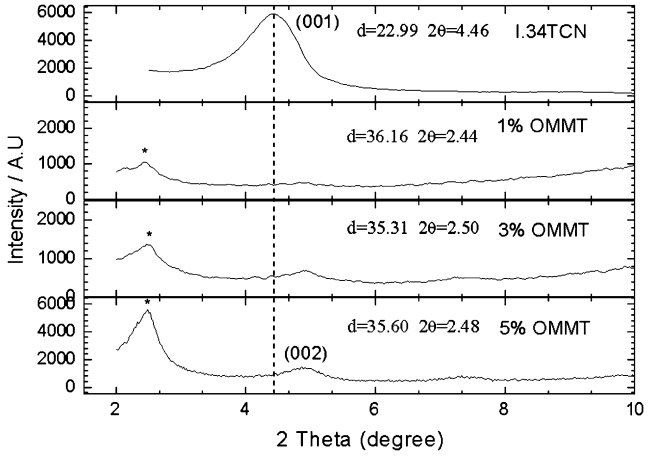

Fig. 5. WAXD patterns of organo-modified montmorillonites (OMMT) powder and PLLA/PCL blends with various contents of OMMT. The dashed line indicates the location of the silicate (001) reflection of OMMT (I.34TCN). The asterisks indicate the (001) peak of OMMT dispersed in a PLLA/PCL blend matrix.

geometrical constraints restrict such high aspect ratio silicate layers exfoliation further, so there is no more improvement in thermal stability, even some decrease, can be observed.

3.3. Microstructure of nanocomposites

WAXD patterns of neat OMMT and PLLA/PCL nanocomposites with 1 wt%, 3 wt% and 5 wt% clay are shown in Fig. 5. The dashed line is the peak position of the OMMT (I.34TCN). Its 2θ value is 4.46° and the gallery distance (d_{001} spacing) is 2.30 nm. For PLLA/PCL/1% OMMT blend, the distance is increased to 3.62 nm ($2\theta = 2.44°$) due to the intercalation of PLLA and PCL. For blends with 3% OMMT, the d_{001} spacing is 3.53 nm ($2\theta = 2.50°$), and for 5% OMMT is 3.56 nm ($2\theta = 2.48°$). The peak becomes higher with the increase of clay content. Small peaks are observed at

Table 2
Thermal stability of PLLA/PCL and its nanocomposites

Samples	$T-80\%$ (°C)	$T-60\%$ (°C)	$T-40\%$ (°C)	$T-20\%$ (°C)
PLLA/PCL	361.4	372.6	381.0	389.3
With 3% OMMT	363.4	375.1	383.3	391.5
With 5% OMMT	372.9	386.9	397.4	407.9
With 7.5% OMMT	369.7	383.8	394.2	404.8
With 10% OMMT	368.0	383.3	393.8	404.2

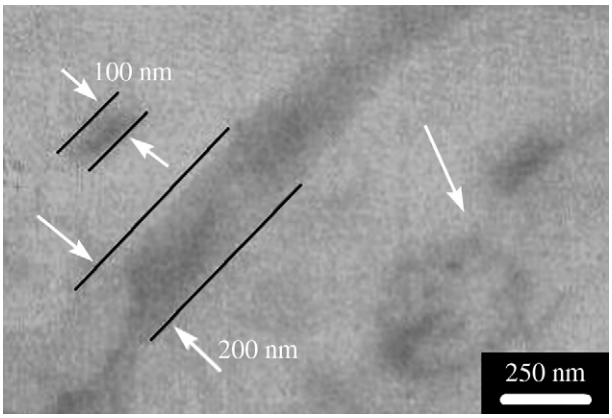

Fig. 6. TEM micrograph of the PLLA/PCL/1% OMMT nanocomposite.

$2\theta \approx 4.86°$ in the case of blends with 3% or 5% OMMT. This is because the (002) plane (d_{002}) of the silicate layers gets dispersed in the polymer matrix. In each blend, polymer chains were intercalated in the silicate galleries, and the coherent order of the silicate layers is much higher with increasing clay content [21]. From this WAXD patterns we can conclude that the ordered intercalated nanostructures are formed in the blends.

Fig. 6 exhibits the TEM image of PLLA/PCL/1% OMMT nanocomposites which shows the best properties and composite effect. Dark bundles of OMMT are dispersed in polymer blends with both intercalated and exfoliated state which can be seen clearly in the image. It was difficult to distinguish the PLLA phase from the PCL domain because there was little contrast difference between them. However, based on the calculation of interaction parameter between PLLA (PCL) and OMMT in Section 3.6, it is reasonable to assume that the OMMT layers are located mainly in the PLLA phase.

3.4. Reduce phase-separated effect of OMMT

Fig. 7 shows the SEM images of the freeze-fracture surfaces of neat PLLA and PLLA/PCL blends with various contents of the OMMT in the same scale. Neat PLLA shows a smooth freeze-fracture surface in image (a). Image (b) shows a blend which has non-uniform particles with large diameter at about 3–4 μm. These particles might be PCL particles in PLLA matrix because as the less content dispersed phase PCL is immiscible with PLLA, or might be the PCL and

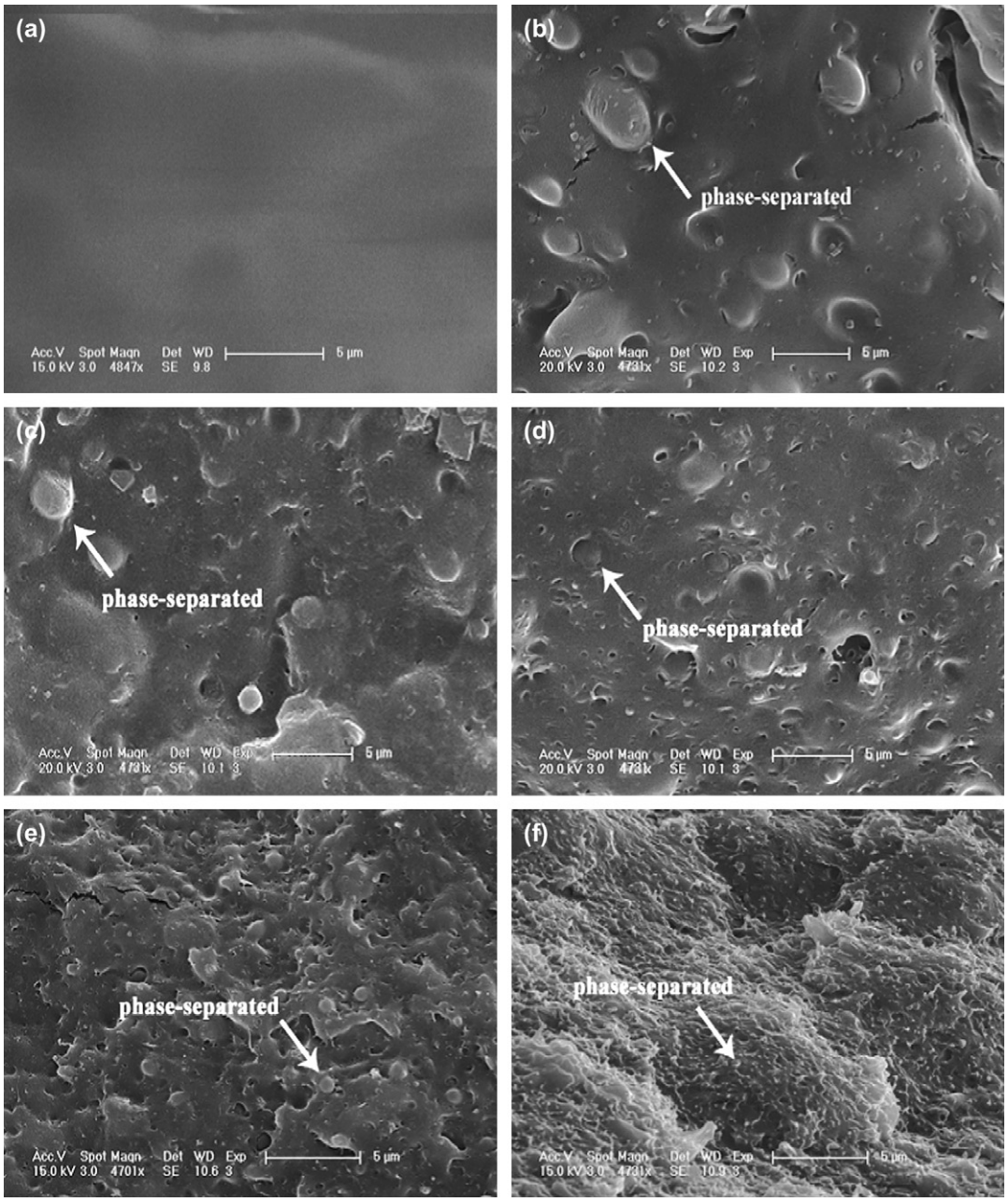

Fig. 7. SEM micrographs of the neat PLLA (a) and PLLA/PCL blends with various amounts of OMMT: (b) 0%, (c) 1%, (d) 3%, (e) 5% and (f) 10%.

PLLA composites. Anyway, this phenomenon is the main reason for poor mechanical properties of the material. Although phase-separated particles also can be seen in images (c) and (d), the size of them has slightly decreased to approximately 2–3 μm. The same trend also can be seen in image (e) in which the average particle diameter is about 1 μm. The addition of 10 wt% of OMMT has resulted in a further decrease in phase-separated particle size to 0.2–0.5 μm, as shown in image (f). From the results listed above, it is quite interesting that OMMT plays a role like compatibilizer, although it is not, as similar reduction phenomenon in phase-separated particle size was reported for triblock PLLA–PCL–PLLA copolymer used as a compatibilizer in similar blend systems [11]. This phenomenon may mainly be due to the intercalation of polymer molecules in OMMT which increases the viscosity ratio and results in the retardation of coalescence of the dispersed phase-separated particles and the enhanced compatibility caused by the intercalation of both PLLA and PCL molecules into the same OMMT gallery [13].

3.5. Thermal parameters of materials

Fig. 8 shows the thermograms of neat PLLA (PCL), PLLA/PCL blend and their nanocomposites with various amounts of OMMT. The thermal parameters of PLLA in blends are listed in Table 3. Because the T_g of PLLA is very close to the T_m of PCL, which can be seen clearly in the DSC thermograms, thermal parameters of PCL in materials cannot be correctly

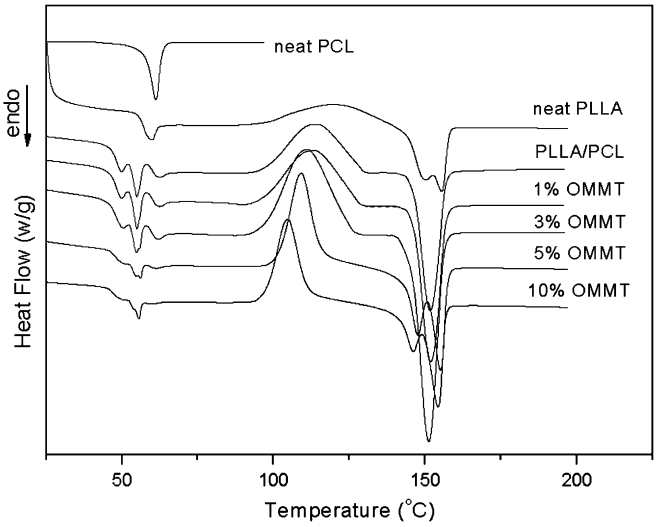

Fig. 8. DSC curves of neat PLLA (PCL), PLLA(90)/PCL(10) blend and with different amounts of OMMT. Experiments carried out under nitrogen flow with a heating ramp of 10 °C/min from 0 °C to 200 °C.

Table 3
Thermal parameters of PLLA in PLLA/PCL blend and in nanocomposites

Sample	T_c (°C)	ΔH_c (J/g)	T_m (°C)	ΔH_m (J/g)	χ_c (%)
PLLA/PCL	113.5	20.1	151.7	16.9	21.3
1% OMMT	113.2	18.1	151.9	19.9	23.9
3% OMMT	111.0	24.5	151.2	22.4	27.5
5% OMMT	109.1	25.1	151.4	24.8	31.1
10% OMMT	104.7	24.1	150.1	22.8	30.4

calculated. The T_g of PLLA is in the same situation. By considering ΔH_m^*, melting enthalpy of 100% crystalline PLLA, as 93.7 J/g [25], we have estimated the value of crystalline degree, χ_c, of PLLA in different systems. χ_c of composites should based on the equation:

$$\chi_c = \frac{\Delta H_m}{(1-\phi)\Delta H_m^*} \times 100\%$$

where ϕ is the weight fraction of filler, including PCL and OMMT, in nanocomposite and ΔH_m is the heat of fusion.

According to the data listed in Table 3, T_c of blends gradually decreases with the increasing content of OMMT while T_m nearly remains steady. This phenomenon has been reported in many other researches [20,21,26]. Also, we can notice that the crystalline peak of nanocomposites becomes sharp with the increasing content of OMMT. In the meantime, ΔH_c increases modestly together with ΔH_m when adding OMMT into blends. These two phenomenons clearly indicate that OMMT in nanocomposites acts as a kind of heterophase crystal nucleation agent. For the first phenomenon, more OMMT can make material crystallization quicker, thus the peak is sharper. While, for the second phenomenon, in lower content of OMMT, polymer in nanocomposite, especially PLLA, seems much easier to form crystals. However, when adding 10% OMMT into blend, melting and crystalline enthalpy values of nanocomposite have decreased a little. This is mainly because more exfoliated layered silicates have restricted the crystallization behavior of PLLA.

3.6. Interaction parameter

Traditionally, the melting point depression phenomenon is found to be explicable in terms of thermodynamic mixing of a crystalline polymer with an amorphous polymer. It is because the crystalline structure of crystalline polymer is diluted by the amorphous polymer [17]. Because the layered structure of clay restricts the formation of crystalline structure of polymer, it can be deduced that layered silicates can play the same role like amorphous polymer in polymer–clay systems, which has been proved by some recent works [15,16]. The melting temperature and the heat of fusion of the polymer/OMMT mixture decrease with the increase of OMMT content, showing that the polymer and OMMT are miscible in the molecular level. The relationship between melting point depression and interaction energy parameter in the mixture can be described by the following well-known Nishi–Wang equation:

$$T_m^0 - T_{mix}^0 = -\frac{BV_{iu}}{\Delta H_{iu}} T_m^0 (1-\phi_i)^2 \quad (1)$$

where T_m^0 and T_{mix}^0 are the equilibrium melting points of the blend PLLA (PCL)/OMMT, respectively. $\Delta H_{iu}/V_{iu}$ is the heat of fusion of PLLA (PCL) per unit volume, and ϕ_i is the volume fraction of PLLA (PCL). B is a function of Flory–Huggins interaction parameter, χ_{12}, they having the following relationship: $\chi_{12} = BV_{iu}/RT$. The overall interaction energy density, B, can be obtained from the slope of the plot of $T_m^0 - T_{mix}^0$ as a function of $(1-\phi_i)^2$.

The equilibrium melting temperatures of pure PLLA and PLLA/OMMT composites are obtained using the Hoffman–Weeks plots (Fig. 9) and the results are listed in Table 4. Fig. 10 shows that the melting point depression of PLLA in the PLLA/OMMT blends depends on the PLLA content. The value of B in Eq. (1) is calculated from the slope of the

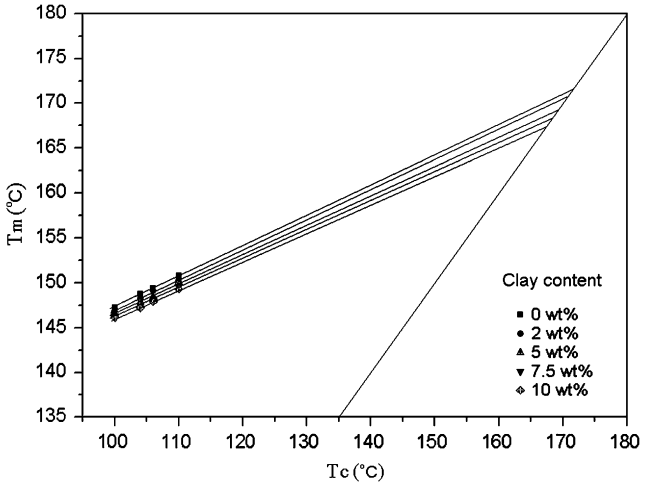

Fig. 9. Hoffman–Weeks plot for the PLLA/OMMT composites with various clay contents.

Table 4
Measured equilibrium melting temperature of PLLA/OMMT blends

PLLA/OMMT (wt/wt)	T_m^0 (°C)	ΔT_m^0 (°C)
100/0	171.6	–
98/2	170.7	0.9
95/5	169.2	2.4
92.5/7.5	168.2	3.4
90/10	167.4	4.2

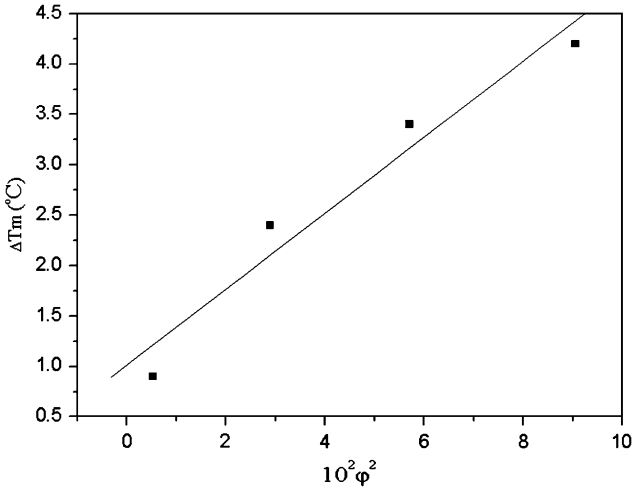

Fig. 10. Plot of equilibrium melting point of PLLA in the PLLA/OMMT composites.

straight line shown in Fig. 10. Considering that the bulk density of PLLA is 1.28 g/cm^3 and that the melting enthalpy of 100% crystalline PLLA is 93.7 J/g [25], the values of V_{iu} and ΔH_{iu} are 1.52×10^5 cm^3/mol and 43.31×10^5 cal/mol, respectively. So the value of PLLA/OMMT interaction parameter B is -6.30 cal/cm^3. The negative value of B for the PLLA/OMMT system indicates that two components can form a thermodynamically stable compatible mixture at temperature above the melting point represented in Eq. (1).

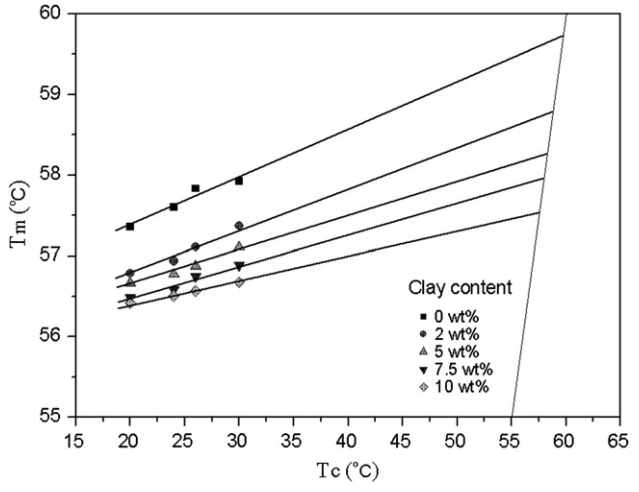

Fig. 11. Hoffman–Weeks plot for the PCL/OMMT composites with various clay contents.

Table 5
Measured equilibrium melting temperature of PCL/OMMT blends

PCL/OMMT (wt/wt)	T_m^0 (°C)	ΔT_m^0 (°C)
100/0	59.7	–
98/2	58.8	0.9
95/5	58.3	1.4
92.5/7.5	58.0	1.7
90/10	57.5	2.2

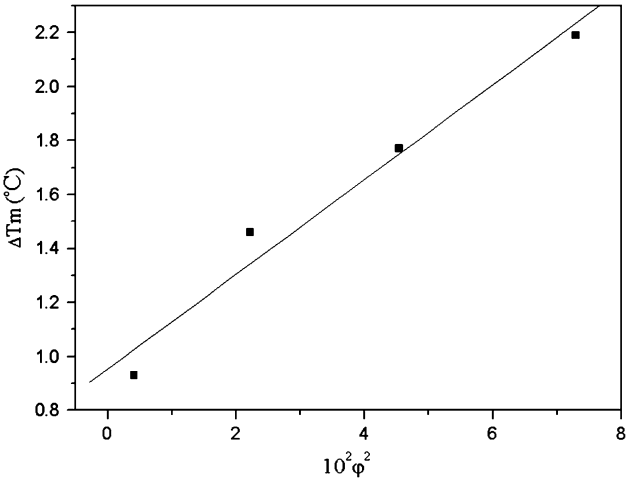

Fig. 12. Plot of the equilibrium melting point of PCL in the PCL/OMMT composites.

The magnitude of the B value indicates that there is a moderate interaction between PLLA and OMMT.

Fig. 11 shows the equilibrium melting temperatures of pure PCL and PCL/OMMT composites and the results are listed in Table 5. In the similar manner as that of PLLA/OMMT composites, the interaction parameter B (-1.08 cal/cm^3) of PCL and OMMT can be obtained, as shown in Fig. 12. The V_{iu} and ΔH_{iu} values are 0.64×10^5 cm^3/mol and 23.32×10^5 cal/mol, respectively.

The interaction parameter of PLLA and OMMT is more negative than that of PCL and OMMT, suggesting that the interaction between PLLA and OMMT is more favorable than that between PCL and OMMT.

4. Conclusions

We have prepared PLLA/PCL/OMMT nanocomposites by melting blend of PLLA, PCL and OMMT. The silicate layers of the clay were intercalated and randomly distributed in the matrix. The addition of OMMT to the PLLA/PCL blend significantly improved the tensile properties and dynamic mechanical properties of nanocomposites. On the other hand, layered silicate explicitly improved the thermal stability of PLLA/PCL blends when the OMMT content is less than 5 wt%. SEM images showed that adding OMMT could decrease the size of phase-separated particles, which made the material more uniform. More OMMT in nanocomposites bring about lower crystalline temperature and higher crystalline

degree. Finally, The interaction parameters, B, were estimated to be -6.30 and -1.08 cal/cm^3 for the PLLA/OMMT and PCL/OMMT system, respectively, indicating that OMMT was more compatible with PLLA.

Acknowledgements

This work was supported by National Natural Science Foundation of China (project number 50473061) and Shanghai Science and Technology Committee (project number 05JC14067). The authors are grateful to Prof. Stanislaw Slomkowski of Polish Academy of Sciences for his helpful ideas and comments throughout this work. We also express our appreciation to the reviewers for their constructive and meticulous assessment of the manuscript.

References

[1] Cai Q, Yang J, Bei JZ, Wang SG. Biomaterials 2002;23:4483–92.
[2] Heller J, Pharma AP, Domb AJ. Adv Drug Deliv Rev 2003;55:445–6.
[3] Formin VA, Guzeev VV. Prog Rubber Plastics Technol 2001;17:186–204.
[4] Yang YF, Wu DX, Li CX, Liu L, Cheng XH, Zhao HY. Polymer 2006;47:7374–81.
[5] Ray SS, Bousmina M. Polymer 2005;46:12430–9.
[6] Riley SL, Okun LE, Prado G, Applegate MA, Ratcliffe A. Biomaterials 1999;41:2245–56.
[7] Fishbein I, Chorny M, Rabinovich L, Banai S, Gati I, Golomb G. J Controlled Release 2000;65(1):221–9.
[8] Kumar R, Bakowsky U, Lehr CM. Biomaterials 2004;25(10):1771–7.
[9] Gogolewski S, Pineda L, Busing CM. Biomaterials 2000;21:2513–20.
[10] Kim K, Yu MK, Zhong XH, Chiu J, Fang DF, Seo YS, et al. Biomaterials 2003;24:4977–85.
[11] Erba RD, Groeninckx G, Maglio G, Malinconico M, Migliozzi A. Polymer 2001;42:7831–40.
[12] Wang L, Ma W, Gross RA, McCarthy SP. Polym Degrad Stab 1998;59:161–8.
[13] Gelfer MY, Song HH, Liu LZ, Hsiao BS, Chu B, Rafailovich M, et al. J Polym Sci Part B Polym Phys 2003;41:44–54.
[14] Wang Y, Zhang Q, Fu Q. Macromol Rapid Commun 2003;24:231–5.
[15] Lim SK, Kim JW, Chin I, Kwon YK, Choi HJ. Chem Mater 2002;14:1989–94.
[16] Chen GX, Kim HS, Kim ES, Yoon JS. Polymer 2005;46:11829–36.
[17] Nishi T, Wang TT. Macromolecules 1975;8:909–15.
[18] Shia D, Hui CY, Burnside SD, Giammelis EP. Polym Compos 1998;19:608–15.
[19] Paul DR, Bucknall CB. Polymer blends: formulation and performance. New York: John Wiley & Sons, Inc.; 2000.
[20] Nam PH, Okamoto M, Kotaka T, Hasegawa N, Usuki A. Polymer 2001;42:9633–40.
[21] Sinha RS, Maiti P, Okamoto M, Yamada K, Ueda K. Macromolecules 2002;35:3104–10.
[22] Ljungberg N, Wesslen B. Biomacromolecules 2005;6:1789–96.
[23] Yin JH, Mo ZS. Modern macromolecular physics, vol. 2. Beijing: Science Press; 2001.
[24] Paul MA, Alexandre M, Degee P, Henrist C, Rulmont A, Dubois P. Polymer 2003;44:443–50.
[25] Hong ZK, Zhang PB, He CL, Qiu XY, Liu AX, Chen L, et al. Biomaterials 2005;26:6296–304.
[26] Krikorian V, Pochan DJ. Macromolecules 2004;37:6480–91.